AAS 24-058

OSIRIS-REX EARTH RETURN & ENTRY: TARGETING STRATEGY AND MANEUVER PERFORMANCE

Daniel R. Wibben[*], Andrew Levine[*], Jason R. Russell[*], Anna T. Montgomery[*], James V. McAdams[*], Samantha Rieger[†], Peter G. Antreasian[*], and Kenneth M. Getzandanner[†]

The OSIRIS-REx sample return capsule landed safely in the Utah desert on September 24, 2023. Starting with the departure from asteroid Bennu in May 2021 through the release of the sample capsule and its arrival at the edge of Earth's atmosphere hours later, this phase of the mission was planned and analyzed thoroughly to optimize the probability of a successful sample return in a large number of nominal and off-nominal scenarios, all while emphasizing spacecraft safety. This paper discusses the spacecraft and sample capsule Earth return and atmospheric entry trajectory design, maneuver analysis, and flight performance, which ultimately helped lead to a successful sample return and initiation of the OSIRIS-APEX extended mission.

INTRODUCTION

The New Frontiers-class Origins, Spectral Interpretation, Resource Identification, and Security–Regolith Explorer (OSIRIS-REx) mission[1] has collected a sample of near-Earth asteroid (101955) Bennu and successfully returned that sample to Earth. After a successful Touch-and-Go (TAG) sample collection in October 2020, the spacecraft stowed the sample in the Sample Return Capsule (SRC) and completed post-TAG observations of the sample site[2] before departing Bennu in May 2021, beginning a nearly ballistic trajectory to return to Earth. Hours before entering Earth's atmosphere, the mission successfully completed a sequence of key events, including SRC release, and landed the capsule in the Utah Test and Training Range (UTTR) on September 24, 2023. The SRC was then retrieved and transported to NASA Johnson Space Center for sample analysis and archival. Shortly after releasing the SRC, the spacecraft bus performed a divert maneuver to safely fly by Earth at an altitude of nearly 800 km and began its extended mission to visit the asteroid Apophis, denoted as the Origins Spectral Interpretation Resource Identification Security APophis EXplorer (OSIRIS-APEX).[3]

The Flight Dynamics System (FDS) team was responsible for the design, modeling, analysis, and implementation of the spacecraft trajectory through the entire mission, up until the point at which the SRC reaches Earth's atmosphere at a location denoted as the Entry Interface (EI), defined at a distance of 6503.142 km from Earth's center. This point is roughly equivalent to an altitude of 130 km, but is not dependent on the sub-spacecraft point in its calculation. At the EI, the Entry, Descent, and Landing (EDL) team took responsibility for the atmospheric descent modeling and

[*]KinetX, Inc. Space Navigation and Flight Dynamics Practice, 21 W. Easy St., Ste 108, Simi Valley, CA 93065, USA
[†]NASA/GSFC Code 595, 8800 Greenbelt Rd, Greenbelt, MD 20771, USA

path prediction of the SRC to the ground, utilizing their high fidelity atmospheric and aerodynamic models.[4]

This paper discusses the design, analysis, and execution of the trajectory used by the OSIRIS-REx FDS team to navigate the spacecraft to the necessary EI conditions. After showing the overall strategy and concept of operations (ConOps) from the Bennu asteroid departure maneuver (ADM) to Earth Return, this paper will describe the method used to derive the entry corridor requirements for the FDS team to evaluate the trajectory prior to the handoff to EDL. Next, the Monte Carlo analysis methodology and results used for the design of this portion of the mission will be presented. The final section includes a detailed evaluation of the actual performance of this strategy comparing the as-flown trajectory and maneuver performance of the successful entry operations with what was planned and analyzed, with specific focus on the final few weeks before Earth atmospheric entry.

TRAJECTORY DESIGN AND ANALYSIS

The Earth Return trajectory was designed to begin with the departure of the spacecraft from Bennu and end with delivery to the Earth EI point in September 2023. In accordance with mission requirements,[5] the trajectory had to remain off of the Earth impact disk (defined as Earth's equatorial radius plus 125 km for Earth's atmosphere) until the final entry targeting maneuvers prior to SRC Release. Thus, the design successively targeted closer flybys of Earth until Entry (E)-14 days, when the final maneuvers targeted the EI point. A high level summary of the propulsive maneuvers and their respective Earth flyby targets is shown in Table 1.

Table 1: Earth Return Maneuver Schedule.

Maneuver	Date	ΔV (m/s)	Target
ADM	10-May-2021	265	10,000 km altitude Earth periapse
ADMa	24-May-2021	-	ADM Cleanup Maneuver
TCM-9	21-Sep-2022	0.25	2,000 km altitude Earth periapse
TCM-10	26-Jul-2023	0.56	200 km altitude Earth periapse
TCM-11	10-Sep-2023	0.24	Earth Entry (Ephemeris Time (ET))
TCM-12	17-Sep-2023	-	TCM-11 Cleanup
TCM-13	23-Sep-2023	-	Earth Entry (Contingency only)
Divert	24-Sep-2023	65.53	$\geq$ 250 km altitude Earth periapse, and enable OSIRIS-APEX extended mission

Earth Return Strategy

The baseline Earth Return trajectory began with the ADM in May 2021. As the first in a series of maneuvers designed to successively target closer Earth flybys in September 2023, the ADM targeted an Earth flyby with a closest approach altitude of 10,000 km. Monte Carlo analysis prior to execution demonstrated that this design resulted in a large distribution of possible trajectories, with approximately 5.75% of these eventually impacting Earth if no additional maneuvers were to be performed. Typically the mission aimed to keep this probability below 1%, the project accepted the additional risk following ADM due to the significant amount of time and number of cleanup opportunities between maneuver execution and arrival at the Earth B-Plane. The nominal cleanup maneuver, ADMa, was scheduled to be performed 2 weeks later, and analysis showed that execution of the cleanup removed any possibility of the spacecraft being on an Earth impact trajectory. In practice, ADM execution placed the spacecraft on a trajectory with a closest approach altitude of 35,000 km, which had only a small impact on subsequent maneuvers and thus no cleanup was necessary. The Earth B-Plane plot from the final ADM Monte Carlo analysis, performed 10 days prior to execution, is shown in Figure 1, with the blue cross in the figure representing the nominal trajectory.

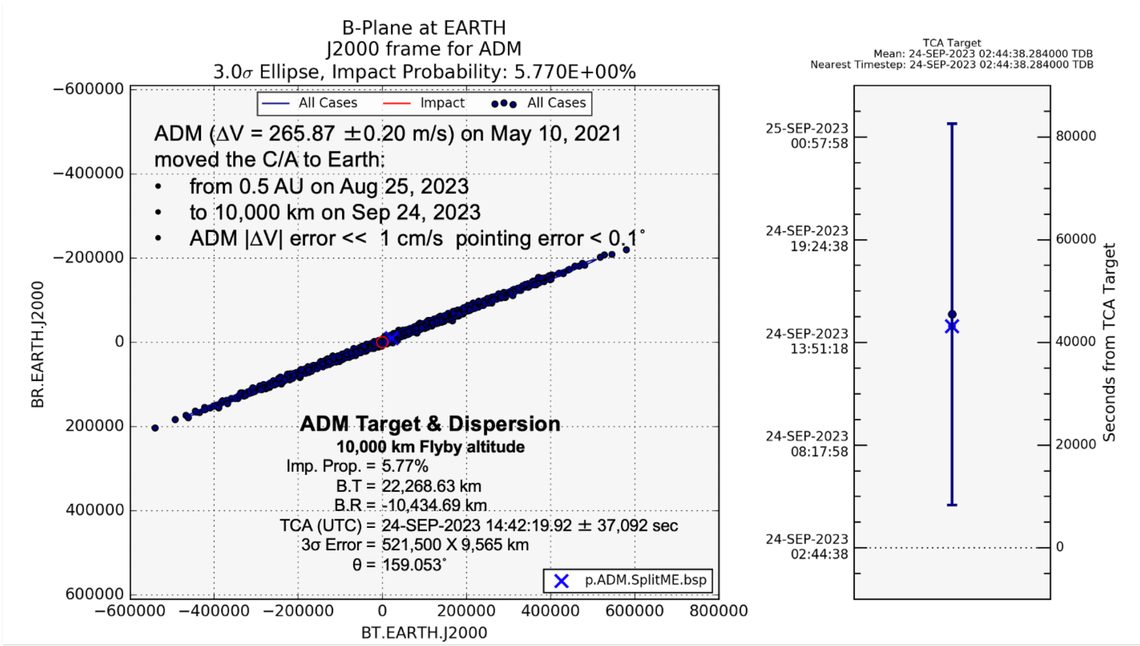

Figure 1: ADM Monte Carlo B-Plane.

The next deterministic maneuver in the return trajectory was Trajectory Control Maneuver (TCM)-9, scheduled on September 21, 2022 and designed to target an Earth flyby with a closest approach altitude of 2000 km, which Monte Carlo analysis showed to be the minimum allowable to provide a less than 1% probability of the spacecraft being on an impact trajectory. Prior to TCM-9, a series of calibration maneuvers of the ACS turn-burn-turn (ACSTBT) and Low-Thrust Reaction Assembly (LTR) thruster suites was performed in the summer of 2022. These calibrations were designed with 3 primary goals:

- ΔV magnitude in the range expected with the final Earth targeting maneuvers in order to confirm the execution error model being used for analysis
- ΔV direction optimized for visibility along the Earth line-of-sight in order to provide the most information possible from radio-metric ranging and Doppler measurements
- Maintain the TCM-9 ΔV magnitude near the level that had been previously analyzed (approximately 25 cm/s)

After the fact, it was discovered that execution of the larger ACSTBT calibration burns altered the spacecraft trajectory enough that it now had a large probability of Earth impact if no future maneuvers were to be performed. TCM-9 was then designed to raise the trajectory and reduce the impact probability back to zero. Subsequent reconstruction of the maneuver showed a slight overburn against the nominal design and resulted in an estimated Earth closest approach distance of 2150 km and an Earth impact probability of zero. The TCM-9 target ellipse from it's final design, and the resulting predicted ellipse (as of OD341, Data Cutoff (DCO) on 11/10/2022) of the Earth B-Plane are shown in Figure 2.

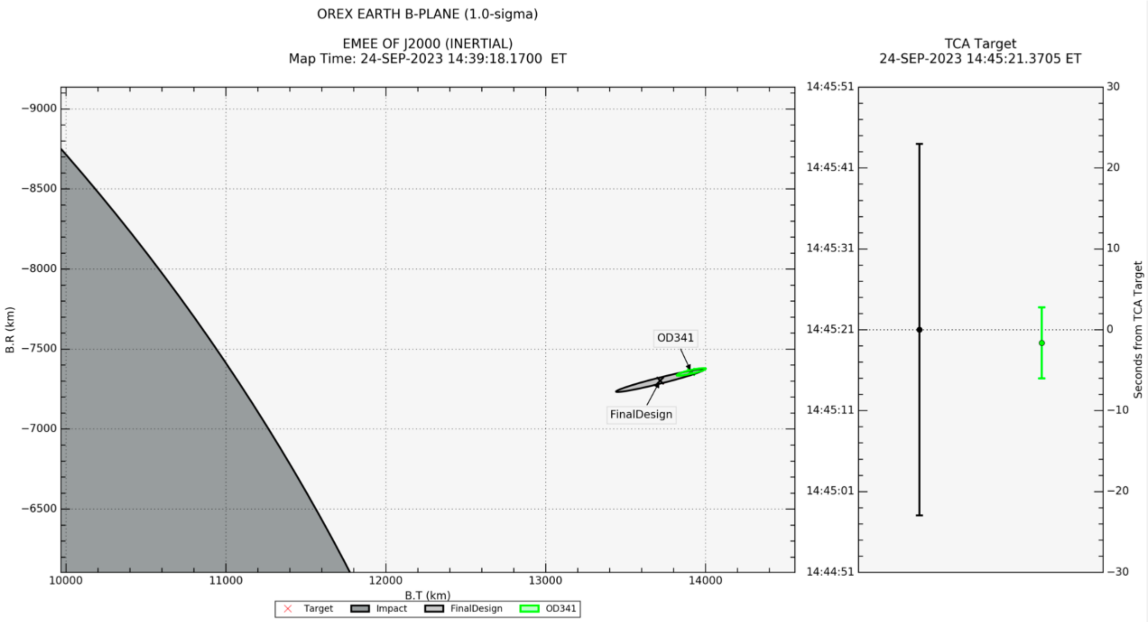

Figure 2: TCM-9 Final Design Predicted and Reconstructed Earth B-Plane.

The maneuver ConOps was designed to walk-in the Earth flyby distance beginning with TCM-10, scheduled for July 26th, 2023 (E-60 days) as shown in Figure 3. TCM-10 was designed to lower the closest approach distance to 200 km, which was again based on Monte Carlo analysis that showed this distance placed less than 1% of cases on an Earth impact trajectory. TCM-11, nominally scheduled at E-14 days as the final deterministic maneuver in the series, was the first maneuver to target the Earth EI point for the SRC, followed by a statistical maneuver, TCM-12, at E-7 days to cleanup any residual error resulting from TCM-11 execution. A contingency-only statistical maneuver, TCM-13, was included in the schedule at E-31 hours. Excepting TCM-13, each maneuver had valid backup opportunities (see Table 2) that were scheduled and analyzed to achieve the targets should any have failed to execute. While FDS analysis showed that valid backup opportunities for TCM-11 and TCM-12 existed for each day beginning at E-14 days, only a handful of these were officially placed in the schedule to help reduce the number of possible scenarios to be analyzed and prepared for.

Table 2: Backup Maneuver Opportunities.

Maneuver	Date	Backup Date 1	Backup Date 2	Backup Date 3
TCM-10	26-Jul-2023 (E-60d)	03-Aug-2023 (E-52d)		
TCM-11	10-Sep-2023 (E-14d)	12-Sep-2023 (E-12d)	14-Sep-2023 (E-10d)	17-Sep-2023 (E- 7d)
TCM-12	17-Sep-2023 (E- 7d)	19-Sep-2023 (E- 5d)	21-Sep-2023 (E- 3d)	23-Sep-2023 (E-31h)

The EI point was selected as the hand-off point between FDS and EDL for generation and analysis of the SRC trajectory and was the target for TCM-11, TCM-12, and if necessary, TCM-13. This EI point was selected to be high enough above Earth's atmosphere that its dynamics do not have a significant impact on the modeling of the SRC trajectory prior to reaching this distance. After EI, the EDL team would utilize their high-fidelity wind and atmospheric modeling to determine the landing location of the SRC at Utah Test and Training Range (UTTR). Their results would be the *de facto* metric for evaluating the success or viability of any trajectory. The formal definition of the nominal entry target is as follows:

- Earth radius of 6503.142 km
- Inertial (J2000) Entry Flight Path Angle (EFPA) of -8.20 deg
- Geocentric Earth latitude of 37.328 deg at 24-Sep-2023 14:43:04 ET
- Earth longitude of 122.812 deg West at 24-Sep-2023 14:43:04 ET

The latitude and longitude values are notably specified at an exact epoch. These values are correlated in order to center the ellipse on the ground at UTTR, and so an adjustment in either of these values will also require a change in epoch and vice versa.

Included in the schedule at E-13 hours was an opportunity to execute one of three possible Conjunction Avoidance Maneuver (CAM) designs. If the nominal trajectory of either the spacecraft bus or SRC showed a significant probability of conjunction with an Earth-orbiting object, the CAM design that minimized the conjunction probability would be selected for execution at this time. The ΔV directions of these maneuvers were all the same and were selected such that the EI conditions specified above were still achieved for the SRC entry trajectory. Instead, execution of a CAM would shift the time at which they are achieved to be earlier by either 0.5, 1.0, or 2.0 seconds in order to reduce the probability of conjunction. For more details on the scheduling and planning of the CAM, please refer to Reference 5.

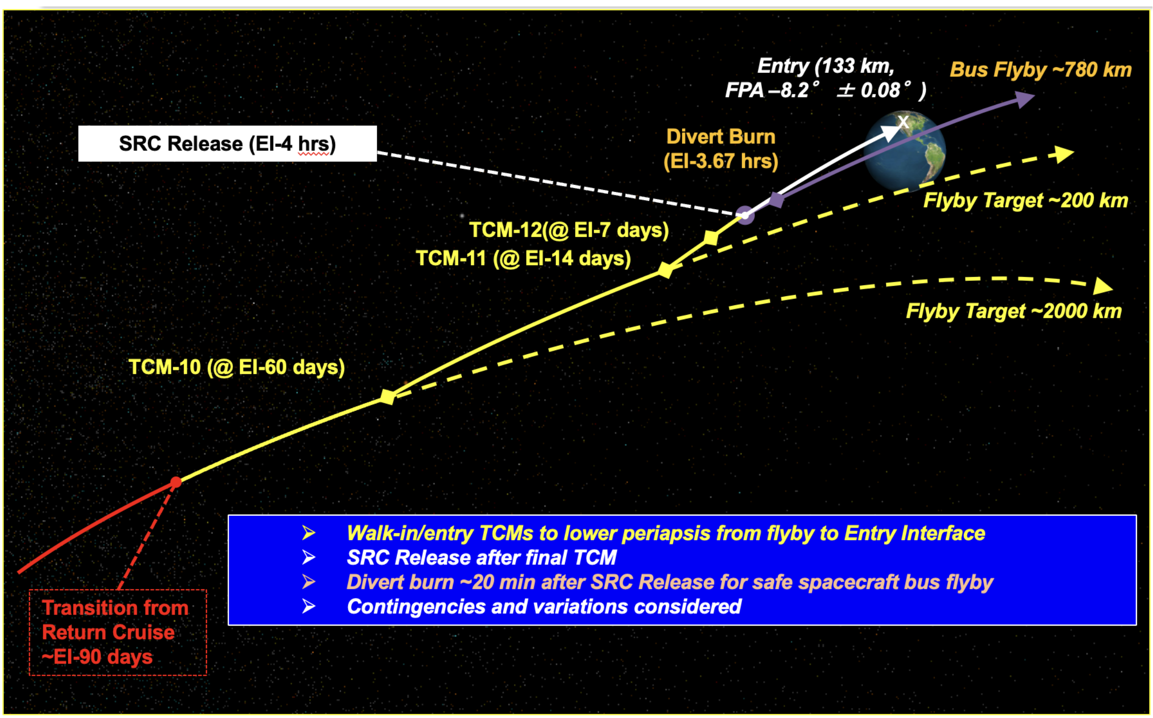

Figure 3: Baseline Earth Return Concept of Operations.

The SRC was scheduled to be released from the spacecraft bus at E-4 hours. The Earth divert maneuver would then be executed 20 minutes after Release to raise the perigee altitude of the spacecraft bus to at least 250 km, per mission requirements. With the later inclusion of the OSIRIS-

APEX extended mission, the design of this maneuver was altered to instead enable the extended mission, provide an Earth perigee altitude of 780 km in the hours following SRC release in 2023, and target a sufficiently biased Earth flyby in September 2025 to guarantee no potential impact with Earth should the spacecraft lose propulsive capability during the two years between Earth encounters.

The execution time of the Earth divert maneuver was tied to the time of release, which in the event of a spacecraft anomaly, could be delayed by up to 1 hour. Because this delay would not be known in advance, beginning with TCM-10 all maneuver designs and analyses included the nominal and 1-hour delayed SRC Release and divert maneuver to ensure a successful SRC landing at UTTR and a safe divert of the spacecraft bus from Earth in both the nominal and worst-case SRC release timing scenarios.

Trajectory Design Process

A design process across multiple tools was exercised prior to ADM as part of a trade study on the desired asteroid departure date. The Evolutionary Mission Trajectory Generator (EMTG) software package provided a ballistic reference trajectory solution that directly targeted the EI point with a ΔV optimized ADM design. The PVDrive Interface and Robust Astrodynamic Target Engine (PIRATE) software tool then provided forward-shooting optimization of the walk-down design with off-Earth biasing to provide the desired flyby distances while minimizing total ΔV. The final trajectory design and maneuver targeting was performed using heritage OSIRIS-REx tools and procedures that had been utilized for operational maneuver and trajectory designs throughout the mission.

In order to protect against any 'unknown unknowns' leading up to Earth encounter, the FDS and EDL teams developed a process to allow for iteration and adjustment of the EI target and the subsequent location of the landing ellipse at UTTR should models or assumptions change. This process was set to be initiated by the EDL team by providing a delta in latitude and longitude to be applied by the FDS team to the existing EI target. The FDS team would apply these shifts, and determine the according shift in time at which the spacecraft reached EI in order to maintain the same EFPA conditions. If the shift showed significant impact on the size of TCM-10 and TCM-11, the PIRATE tool remained available in order to reoptimize the trajectory to help reduce the ΔV of these maneuvers. After execution of TCM-10, large shifts would not be allowed though smaller shifts would still be available so long as the thruster suites for each maneuver remained consistent (to avoid complications with spacecraft commanding), and analysis of the new trajectory showed all requirements were still being met. The updated trajectory would then be provided to the EDL team in order to confirm the shift was applied correctly and appropriately aligned the landing location at UTTR. If more adjustment was necessary, the two teams would iterate until the landing location was fully adjusted. This iterative process, as well as many other processes and procedures, were tested and validated via two Operational Readiness Tests executed in mid-2023.[5]

Predicted Spacecraft Attitude

The spacecraft attitude was primarily Sun-pointed during this period, with both solar arrays holding a fixed orientation. The predicted attitude model throughout Earth Return included 2, 5-hour high-gain antenna (HGA) passes per week where the spacecraft slewed to an Earth-point orientation. After a commanded reset of the spacecraft onboard processor on August 8, 2023, the spacecraft remained in sun-point continuously. Starting at E-31 hours, the spacecraft switched to the

SRC Release attitude, which was defined to minimize the expected angle-of-attack when the SRC encounters Earth's atmosphere. This attitude was held inertially fixed until 24 hours after Earth divert.

While this orientation was optimized to benefit the dynamics of the SRC, it did also place the Sun high up on the side of the spacecraft which held all science instruments, and the SRC. Earlier in the mission, the team placed the spacecraft in similar Sun-relative orientations and observed outgassing due to sublimation of frozen water held within the shell of the SRC.[6] The team expected additional outgassing when returning to this orientation, but analysis showed its impact would be negligible, thus no explicit model was included in the trajectory design.[7]

Prior to July 2023, all analysis of Earth return utilized the SRC Release attitude as defined from pre-launch design and analysis. However, later analysis by the EDL team showed that the attitude definition required updating just before TCM-10 execution. This attitude update was found to be on the order of 5 degrees and was due to a change in the date of ADM from the pre-launch assumed date in March 2021 to the actual executed date two months later. The asteroid departure date was changed both in order to save approximately 20 m/s of ΔV and to provide time to enable the Post-TAG observations at Bennu. However, this change altered the capsule's velocity azimuth at Entry interface by approximately 5 degrees and thus the update was necessary to fix this known offset. Adjusting this attitude definition resulted in a slight change in the TCM-11 design, on the order of 1 cm/s.

Thermal Re-radiation

A model for the acceleration due to thermal re-radiation was derived based on the predicted spacecraft attitude. This is consistent with the strategy utilized throughout the mission and has been discussed in detail in previous work.[8]

SRC Properties

After separation, the mass of the SRC, including an estimate of the Bennu sample, was assumed to be approximately 50 kg. Its shape and optical properties were unchanged from the full spacecraft as it was assumed that the influence of solar radiation pressure (SRP) and thermal re-radiation were negligible for the 4-hour propagation between SRC release and arrival at EI.

SRC Release

The impact of the release mechanism on the SRC was modeled as an impulsive maneuver, with a ΔV magnitude of 35.24 cm/s relative to the spacecraft bus. This value was based on data derived from an Adams model analysis run by Lockheed Martin (LM) in 2015. Assuming masses of 50 and 1190 kg for the SRC and bus respectively, the conservation of momentum results in inertial ΔV magnitudes of 33.8 cm/s on the SRC and 1.48 cm/s on the spacecraft bus. The direction of the ΔV vector was primarily along the spacecraft +Z axis while in the SRC Release attitude, and in the opposite direction for application of the kickback to the spacecraft bus.

Nominally the release ΔV would be executed four hours prior to predicted arrival of the SRC at EI. In the event of a spacecraft anomaly, this time could be delayed up to an hour. This limit was chosen as an upper-bound per direction from the LM spacecraft team based on the most likely anomalies that could occur in this timeframe. If the hour limit were reached and the SRC was still not released, the spacecraft would perform the Earth divert maneuver with the capsule still attached.

A backup trajectory, which returned the spacecraft to Earth in September 2025 for another attempt, was analyzed by the team and determined to be valid at a preliminary level.

B-PLANE CORRIDOR DEFINITION

While the iterative process between the FDS and EDL teams was established as part of the ConOps to confirm a given maneuver or trajectory design met landing requirements, an entry corridor definition was necessary for the FDS team to understand whether entry requirements were being met without needing to directly involve the EDL team with each trajectory solution. This corridor would need to be based on the landing ellipse requirements as well as the EFPA and would be valid at the EI point. The most convenient form in which to define this corridor is the B-Plane,[9] which was also used in previous Mars EDL missions.[10] Using the B-Plane is also convenient due to the direct mapping between EFPA (γ) and $|B|$, which is defined as:

$$|B| = \frac{RV\cos\gamma}{v_\infty} \tag{1}$$

where R and V are the position and velocity magnitudes, and v_∞ is the magnitude of the asymptotic inbound velocity. This relationship can be used with the requirements on γ to easily define 2 concentric circles in the B-Plane, yet this only constrains one dimension. Additional constraints are necessary to define the acceptable corridor in which the SRC should be delivered to arrive within the defined allowable landing ellipse on the ground. Recent atmospheric entry missions (MSL, Mars 2020) defined a fixed distance value for the cross-track delivery error requirements[10, 11] in order to create an entry corridor 'box'. These cross-track values were determined by the EDL team based on the capabilities of the entry guidance but in this instance the SRC trajectory was entirely ballistic once released from the spacecraft bus. Our approach instead defined a full 6x6 state covariance matrix based entirely on mission and landing ellipse requirements, and then mapped that in to the B-Plane parameters to provide a full ellipsoid corridor.

State Vector and Requirements Definition

In order to determine the requirements in typical B-Plane coordinates ($B.R$, $B.T$, and Linearized Time of Flight (LTOF)), we first had to define a full state vector with allotted delivery requirements. In addition to the primary mission requirement of $\gamma = -8.2 \pm 0.08$ deg, the spacecraft position and velocity magnitudes could be easily defined. The former was set per the definition of the EI with a variation of zero. The velocity magnitude was set by execution of the Bennu ADM and is essentially constant for all possible trajectories arriving at Earth, with minor variability on the order of under 10 cm/sec. To complete the definition of the velocity state, the heading angle (or velocity azimuth), χ, was introduced, which can be determined by expressing the velocity vector in an East-North-Up coordinate frame:

$$\bar{v}_{ENU} = V_{mag} \begin{bmatrix} \cos\gamma\sin\chi \\ \cos\gamma\cos\chi \\ \sin\gamma \end{bmatrix} \tag{2}$$

There was no explicit mission requirement provided for χ, but the ± 0.08 deg used for γ was used as a proxy since previous analysis demonstrated that the variability in both angles were nearly equivalent.

Finally, requirements on the Earth geodetic body-fixed latitude and longitude, ϕ and λ respectively, had to be defined based on the reference landing ellipse. This ellipse was defined as the negotiated area within which the SRC was allowed to land within UTTR. The mapping of this ellipse up to the equivalent values at the B-Plane was done analytically by comparing the variations observed at the EI point against what was observed on the ground in previous analysis, since a direct mapping between the two was not available. This scaling was then applied to the reference landing ellipse, and the resulting dimensions and orientation were used to retrieve the 2x2 covariance matrix at EI by reverse solving the eigenvalue problem.

Thus the following state vector was used, with each state parameter having a known error budget:

$$\bar{X} = [\lambda, \phi, R_{mag}, V_{mag}, \gamma, \chi] \tag{3}$$

Full State Covariance

While individual requirements on each parameter listed above have been defined, at this point no correlations have yet been defined between each of these parameters except between λ and ϕ, whose correlation was provided from the reference landing ellipse. Approximations of the correlation coefficients between each state parameter could be found by looking at the delivery covariance from previous results. However, further analysis of the covariance and the mapping described in the next section demonstrated that many of the correlations are near 0 (such as between λ and V), and more importantly, that the mapping to the B-Plane is not at all sensitive to many of the missing correlations. In fact, the only correlations that have any significance in the mapping are between ϕ and γ, and ϕ and χ. Thus the full state covariance to be mapped takes the following form:

$$C = \begin{bmatrix} \sigma_\lambda^2 & \rho_1\sigma_\lambda\sigma_\phi & 0 & 0 & 0 & 0 \\ \rho_1\sigma_\lambda\sigma_\phi & \sigma_\phi^2 & 0 & 0 & \rho_2\sigma_\phi\sigma_\gamma & \rho_3\sigma_\phi\sigma_\chi \\ 0 & 0 & 0 & 0 & 0 & 0 \\ 0 & 0 & 0 & \sigma_V^2 & 0 & 0 \\ 0 & \rho_2\sigma_\phi\sigma_\gamma & 0 & 0 & \sigma_\gamma^2 & 0 \\ 0 & \rho_3\sigma_\phi\sigma_\chi & 0 & 0 & 0 & \sigma_\chi^2 \end{bmatrix} \tag{4}$$

As mentioned previously, ρ_1 is obtained from the orientation of the landing ellipse on the ground. The remaining correlation coefficients, ρ_2 and ρ_3, were analytically determined from previous Monte Carlo analyses delivery errors to be 0.96 and 0.91, respectively.

Mapping to the B-Plane

With a full state covariance matrix representing the required errors on each state parameter in hand, the covariance can be linearly mapped to the B-Plane using the partial derivatives of each B-Plane parameter with respect to the state vector, $\bar{X}$.

$$C_B = JCJ^T = \left(\frac{\partial\,(B.R, B.R, LTOF)}{\partial\bar{X}}\right) C \left(\frac{\partial\,(B.R, B.T, LTOF)}{\partial\bar{X}}\right)^T \tag{5}$$

The entry corridor on the B-Plane can be constructed as an ellipse, with the linearized time of flight uncertainty using the usual methods from the eigenvalues and eigenvectors of C_B.[9]

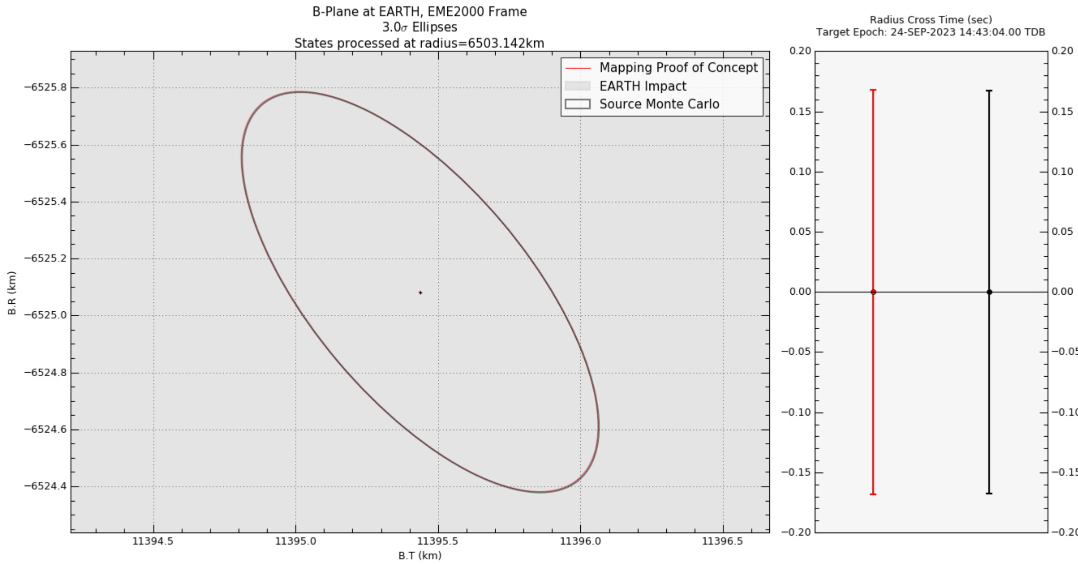

Figure 4: Initial B-Plane corridor proof of concept - matching Monte Carlo results.

Sample Results

The above method was first used with existing Monte Carlo analysis results as a proof of concept. In order to confirm the mapping and partial derivatives were correct, the σ values defining the input covariance C were pulled directly from the Monte Carlo results instead of the requirements as described. The result of the mapping was expected to exactly produce the 3σ B-Plane ellipse as pulled directly from the B-Plane states from the Monte Carlo analysis. This proof of concept was confirmed, as shown in Figure 4 with the generated ellipse and $LTOF$ uncertainty exactly matching the analytical results from the Monte Carlo. The next step was to generate C exactly as specified and compare with the $|B|$ contours which are calculated from Eq. 1. A correct mapping through the process described above was expected to produce an ellipse that fits within these contours and is tangent to them along the axis of the resulting ellipse. This confirmation is shown in Figure 5, where the red ellipse represents the entry corridor when mapped directly from mission requirements.

Later in operations, project management and personnel at UTTR negotiated to define a reference landing area, which represented the true area in which the SRC was cleared to land. The intent was to define an area in which the project would receive automatic concurrence from UTTR if the predicted SRC landing ellipse fell within its boundary. The resulting B-Plane corridor mirroring the negotiated reference landing area is shown in yellow in Figure 5, which notably falls outside the $\pm 0.08°$ EFPA contours. This excursion above mission requirements was deemed acceptable following analysis of the capsule and expected entry conditions, which determined that the capsule could still meet all EDL safety metrics with up to $\pm 0.2°$ EFPA error. This reference landing area was the primary landing deliverability metric used in all decisional meetings in the days leading up to Earth Entry. Thus all results presented throughout the rest of this paper will utilize the reference landing area as the definitive entry corridor as opposed to the original mission requirements.

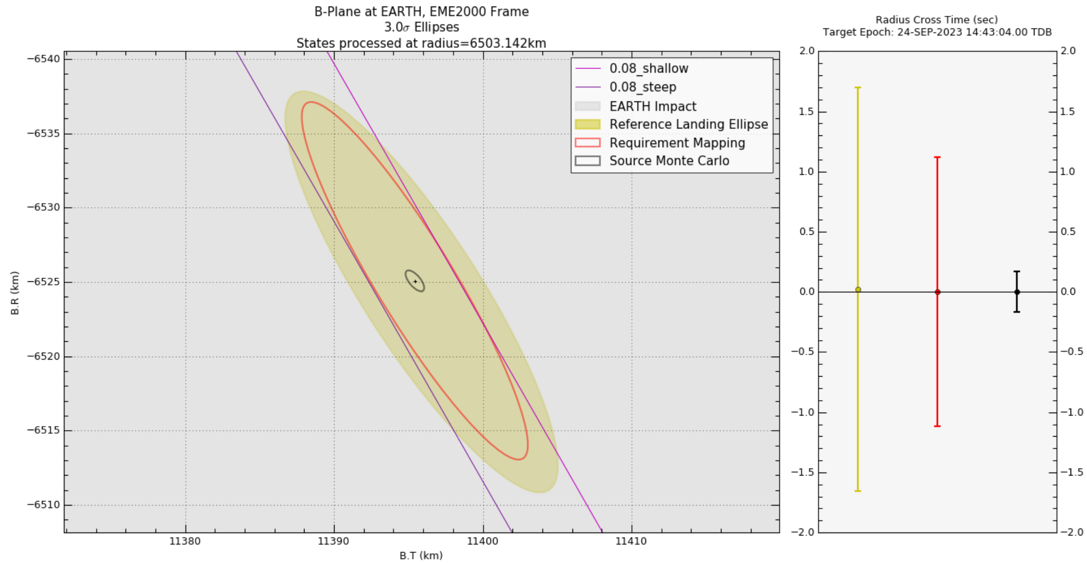

Figure 5: B-Plane corridor proof of concept - matching $|B|$ contours. Requirement ellipse is in red while the final negotiated reference landing ellipse is in yellow.

MANEUVER DESIGN AND ANALYSIS

Monte Carlo Strategy

Monte Carlo analysis was used extensively throughout this phase to ensure that the SRC was on a ballistic Earth entry trajectory within the defined corridor and that the spacecraft bus received a proper gravity assist to place it on target to begin the extended OSIRIS-APEX trajectory to the asteroid Apophis. The general Monte Carlo methodology for maneuvers, depicted in Figure 6, was mostly the same with some variations for targeting and contingency considerations.

The most notable deviation from the core Monte Carlo methodology was that TCM-12 will not be executed if, after TCM-11, the 'commanded' ΔV was above the determined threshold of 1.5 mm/s. This threshold, larger than the minimum executable ΔV of 0.08 mm/s on the LTR thrusters, was determined based on the expected predicted spacecraft velocity uncertainties. Additionally, the statistical nature of TCM-12 resulted in a non-zero probability that the maneuver attitude required to achieve the target would result in placing the instrument deck in a solar illumination condition within the Sun keep-out zone (KOZ) which must be avoided in order to protect the instruments. In the past, this scenario had been remedied by 'decomposing' the maneuver in to a linear combination of two maneuvers which provided a resultant ΔV vector along the original desired direction. The expected ΔV magnitude of TCM-12 maneuvers were below the allowable ACSTBT threshold and therefore were planned to be executed on the LTR thrusters which do not support this decomposition method. A 'pseudo-decomposition' algorithm was derived such that rather than splitting a maneuver into two segments to avoid the Sun KOZ, it chose the closest location on the edge of the KOZ to execute a single maneuver and scaled the ΔV to best approximate the effect of the designed maneuver and minimize the impact of the maneuver being performed in a non-optimal direction.

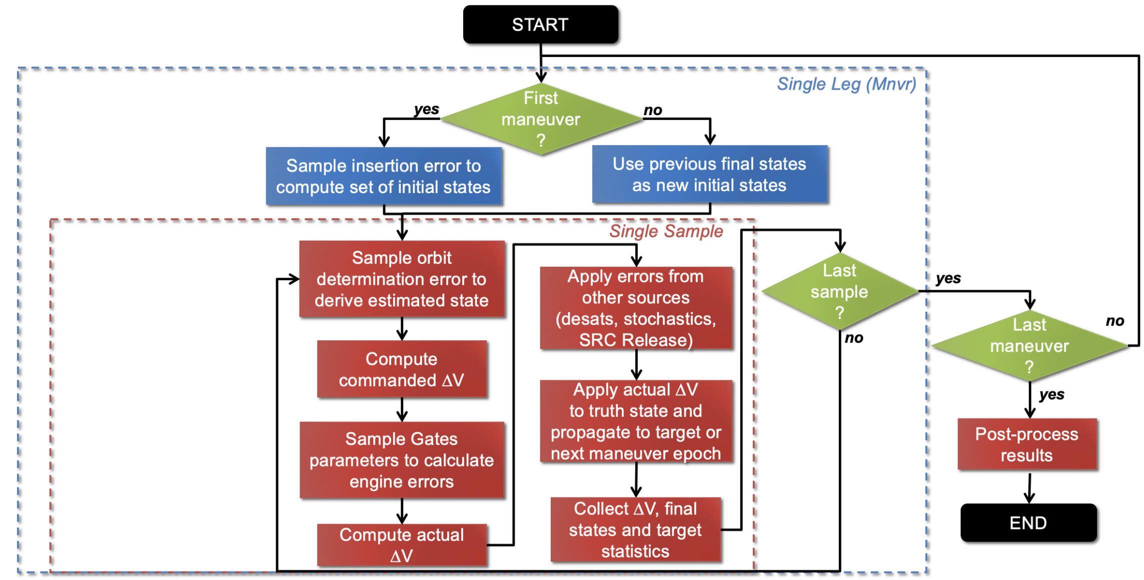

Figure 6: Monte Carlo Analysis Methodology for TCMs (Except TCM-12).

Monte Carlo Analysis Inputs

The thruster execution error models, provided by LM, represent the latest in-flight performance analysis of the ACSTBT, LTR, and TCM thruster suites and were generated based on previous performance of the vehicle in flight over the past seven years. The applicability of these models after the significant mass reduction following execution of the ADM for the ACSTBT and LTR thrusters were confirmed with execution of the calibrations in Summer 2022. The only exception was the execution error model assumed for the Earth divert burn. Due to the timing of the divert relative to SRC Release, the more conservative pre-launch vehicle requirement models were used instead of any model informed by actual flight performance.

The initial condition states are dispersed by sampling the orbit determination (OD) covariance representing the navigation knowledge at the DCO times prior to each maneuver: TCM-9 used a DCO nine days prior to maneuver execution (M-9), TCM-10 used M-7 day DCO, TCM-11 and TCM-12 assumed M-2 day DCO. A variety of OD covariance analysis cases were utilized, with the best-case current best estimate (CBE) scenario representing the data weighting and stochastic acceleration modeling assumed in the current operational OD at that time. The worst-case scenario analyzed represented a contingency scenario in which the entirety of the Canberra DSN complex was unavailable for the months of August and September 2023. While not presented in detail here, this worst-case analysis showed 98.2% of cases satisfied the EFPA requirements, which while still high, violated the 99.7% mission requirement.

The Monte Carlo also included residual ΔV applied to the spacecraft through execution of reaction wheel momentum desaturation events (known as desats), with the last such event occurring 90 minutes after TCM-11.

The SRC release ΔV applied was sampled from a data set provided by LM, which was generated based on test data of the release mechanism under two different thermal conditions, labeled 'ambient' and 'cold', performed prior to launch. The data provided allowed for separate random draws of both the axial error (along the release ΔV direction) and lateral errors in the orthogonal directions. The nominal analysis assumed more conservative assumptions that covered all test data under both thermal conditions, while CBE analysis used only the 'ambient' conditions that were expected to be more likely in flight.

Finally, the Monte Carlo analyses included zero-mean Gaussian stochastic accelerations applied periodically throughout the trajectories to account for any unmodeled or mismodeled forces.

Monte Carlo Analysis Results

The Monte Carlo results provided statistical insight for the team with the final planning of the Earth return activities, and helped prepare for a number of possible challenging contingency scenarios that may have arisen. Foremost, the ΔV statistics from the nominal Monte Carlo case allowed the operations team to confidently choose which thruster suite would best support each maneuver, as indicated in Table 3. The 99% ΔV budget helped to bound remaining propellant mass for future activities such as a missed release contingency or extended mission planning. This table also showed that none of the pre-SRC release maneuvers would violate the Sun KOZ (after application of the previously mentioned 'pseudo-decomposition' algorithm for TCM-12).

Table 3: Nominal Pre-SRC Release ΔV Statistics.

Maneuver	Date	Thruster Set	Deterministic [cm/s]	Mean [cm/s]	SD [cm/s]	1% [cm/s]	99% [cm/s]	Mean Sun Angle [deg]	Decomp %
TCM-9	21-Sep-22	ACSTBT	26.56	26.57	0.36	25.77	27.43	52.44	0
TCM-10	26-Jul-23	ACSTBT	56.99	56.88	2.39	511.41	62.46	147.31	0
TCM-11	10-Sep-23	ACSTBT	23.89	24.03	0.16	20.36	27.76	58.98	0
TCM-12	17-Sep-23	LTR	-	0.51	0.24	0	1.13	92.87	0
DB1	24-Sep-23	TCM	65.21	65.16	0.27	64.54	65.77	114.98	0

The targeting process for TCM-9 and TCM-10 required a less than 1% Earth impact probability, ensuring that TCM-11 was the first maneuver in which the spacecraft's B-Plane probability ellipse could intersect Earth's impact radius. The B-Plane delivery ellipses for TCM-9 and TCM-10 from analysis performed three months prior to TCM-9 execution are shown in Figure 7 and demonstrate Earth impact probabilities below 1%, meeting the mission safety requirements. The TCM-9 and TCM-10 B-Plane ellipses and LTOF details from this analysis are provided in Table 4. TCM-11 and TCM-12 were both targeting the Earth EI, placing the spacecraft's B-Plane ellipse within Earth's impact radius. Figure 8 shows these ellipses from the initial analysis of the return trajectory design against the reference landing area B-Plane corridor and EFPA contours, as defined previously. From this initial analysis, approximately 85% of trajectories were predicted to meet the EFPA requirements after execution of TCM-11. After execution of the TCM-12 cleanup maneuver, this result was improved to 99.96%, demonstrating that the design would meet mission requirements. Full details of the delivery errors for TCM-11 and TCM-12 from this analysis are provided in Table 5.

Another useful result from Monte Carlo analysis is understanding the sensitivities of the delivery error at EI to the various error sources discussed in the previous section. This can be done by performing a series of Monte Carlo analyses with only a single error source included in order to understand the contributions of each source individually. A summary of the sensitivities both at

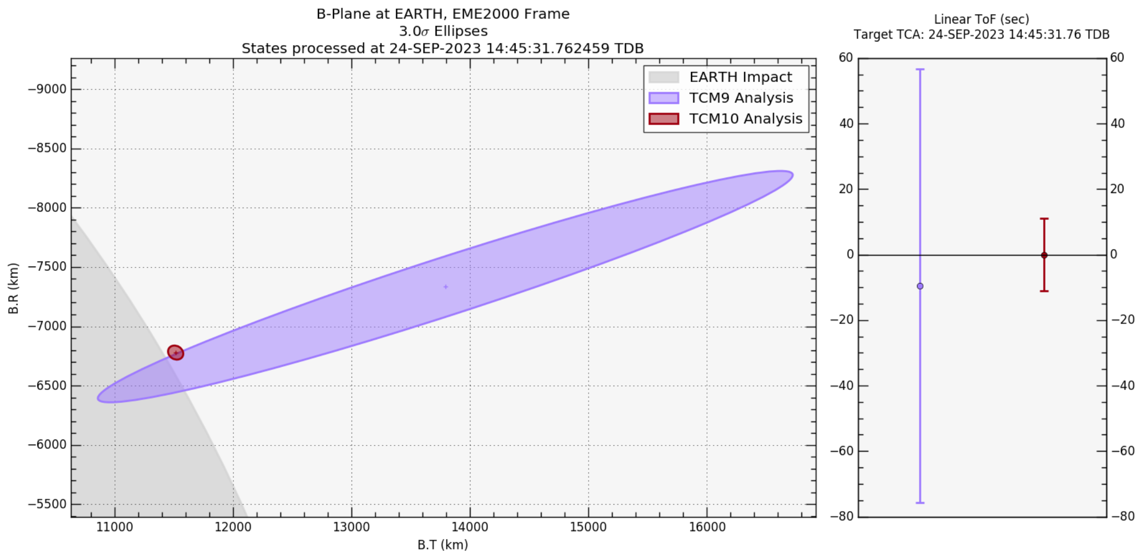

Figure 7: TCM-9 & TCM-10 B-Plane Delivery Ellipses. Analysis performed 3 months prior to TCM-9 execution.

Table 4: Nominal TCM-9 and TCM-10 B-Plane Ellipse Details.

Maneuver	a [km]	b [km]	Orient [deg]	LTOF [sec]	Impact Prob [%]	Target
TCM-9 TCM-10	2295.163 67.108	230.441 56.022	163.800 122.066	67.70 0.86	0.07 0.00	2,000 km Earth flyby altitude 200 km Earth flyby altitude

Table 5: Nominal TCM-11 and TCM-12 Delivery Uncertainty (3-sigma).

Maneuver	Entry Time [sec]	EFPA [deg]	Latitude [deg]	Longitude [deg]
TCM-11 TCM-12	3.128 1.228	0.184* 0.073	0.114 0.045	0.318 0.125

* Falls within ±0.2° EDL safety metric

the time of TCM-11 and TCM-12 are included in Table 6. The numbers in this table represent the percent contribution from each individual error source to the overall delivery error, with 1 representing the error level seen in the full Monte Carlo analysis with all error sources included, and 0 representing no error. Most error sources were described in the previous section, but a few require additional explanation:

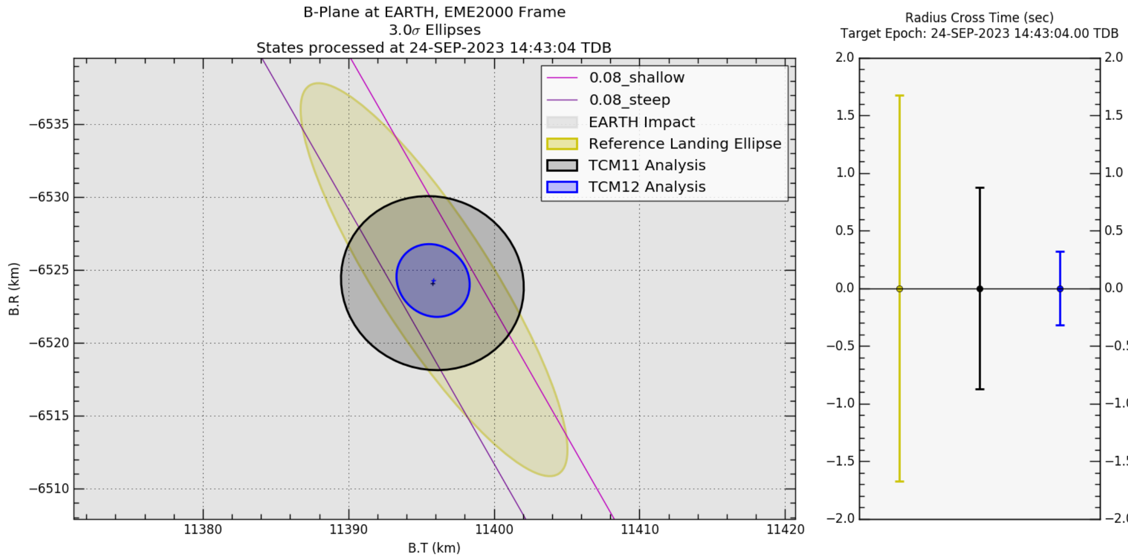

Figure 8: TCM-11 & TCM-12 B-Plane Delivery Ellipses. Analysis performed 3 months prior to TCM-9 execution.

- OD Knowledge - How well the predicted spacecraft state is known at the time of the maneuver from the final design DCO.
- Desat - Error due to the residual ΔV applied by execution of a desat. The final desat is performed 90 minutes after TCM-11, so this is not applicable to TCM-12.
- Waive-Off - Error due to TCM-12 maneuver designs with a ΔV magnitude below 1.5 mm/s being waived off.
- Decomp - Error due to application of the 'pseudo-decomposition' algorithm being applied for the TCM-12 cases that violated the KOZ.

Table 6: EI delivery error sensitivities to various Monte Carlo input error sources, represented as % of the delivery error from the full analysis

Maneuver	Target	OD Knowledge (%)	Maneuver Exec. Error (%)	SRC Release (%)	Stochastics (%)	Desat (%)	Waive-Off (%)	Decomp (%)
TCM-11	EFPA	72	24	16	12	63	-	-
	Latitude	72	23	17	12	64	-	-
	Longitude	72	25	16	12	63	-	-
TCM-12	EFPA	96	16	43	12	-	29	17
	Latitude	91	16	40	11	-	33	29
	Longitude	96	16	43	12	-	30	13

Monte Carlo Analysis during Operations

During the last two weeks leading up to Earth Return, the FDS and EDL teams had to be prepared to deliver multiple Monte Carlos each day in order to inform the project on the possible landing locations corresponding to different potential scenarios. Each day after TCM-11 execution included a 'No Burn', which showed based on the current day's knowledge where the capsule could land if no additional maneuvers were performed. Prior to TCM-12 execution, each day also included a case where the latest maneuver design was included to confirm it reliably corrected back to the nominal target. For each of these scenarios, an added case that delayed the SRC Release by the maximum of 1 hour was included, which served as an upper bound on where the capsule would land should the capsule release not occur at the nominal time. In the final days before SRC Release, the CAM cases were added in to the list of scenarios in order to predict the landing location in the event one of the CAMs was deemed necessary. A summary of the cases run each day is provided in Table 7. Notably, the analyses performed on E-10 days included 2 additional scenarios to look at the impact of using a new target for the TCM-12 design, which will be discussed more in the next section.

Table 7: Monte Carlo Cases Run Per Day in Operations.

Case (below) / Days from EI $\Longrightarrow$	E-16d	E-13d	E-12d	E-11d	E-10d	E-9d	E-8d	E-6d	E-5d	E-4d	E-3d	E-2d	E-1d
TCM-11 With Burn	X												
TCM-11 With Burn + Delayed Release	X												
TCM-12 With Burn	X	X	X	X	X	X	X						
TCM-12 With Burn + Delayed Release	X	X	X	X	X	X	X						
No Burn		X	X	X	X	X	X	X	X	X	X	X	X
No Burn + Delayed Release		X	X	X	X	X	X	X	X	X	X	X	X
0.5 sec CAM											X	X	
1.0 sec CAM											X	X	
2.0 sec CAM											X	X	X
Others					X								
Total	4	4	4	4	6	4	4	2	2	2	5	5	3

FLIGHT PERFORMANCE

While the full return cruise trajectory beginning with Bennu departure affected the overall performance of the return of the SRC, this section will focus on the last two maneuvers, TCM-11, and TCM-12, and the critical events during the last few weeks before Earth Entry.

Following the execution of TCM-10 at E-60 days and the spacecraft reboot at E-47 days, the preliminary design of TCM-11 was performed on August 28 (E-27 days). As mentioned previously, TCM-11 was the primary maneuver designed to change the spacecraft trajectory from an Earth flyby to a trajectory that targets SRC entry conditions. The target conditions for this maneuver were identical to those described previously in this paper, and those used in all analysis described thus far. The OD solutions remained quite stable throughout this period, and the final design delivered on September 8 (E-16 days) showed only slight adjustments to the maneuver parameters, as shown in Table 8. The B-Plane for this design and its 3-sigma Monte Carlo delivery error ellipse is shown against the reference landing ellipse in Figure 9.

The TCM-12 designs were set to be delivered in the week following TCM-11 execution, with the preliminary design delivered on September 11 (E-13 days) and the final on September 15 (E-9 days). With the preliminary design just a day after TCM-11 execution, other than an initial TCM-11

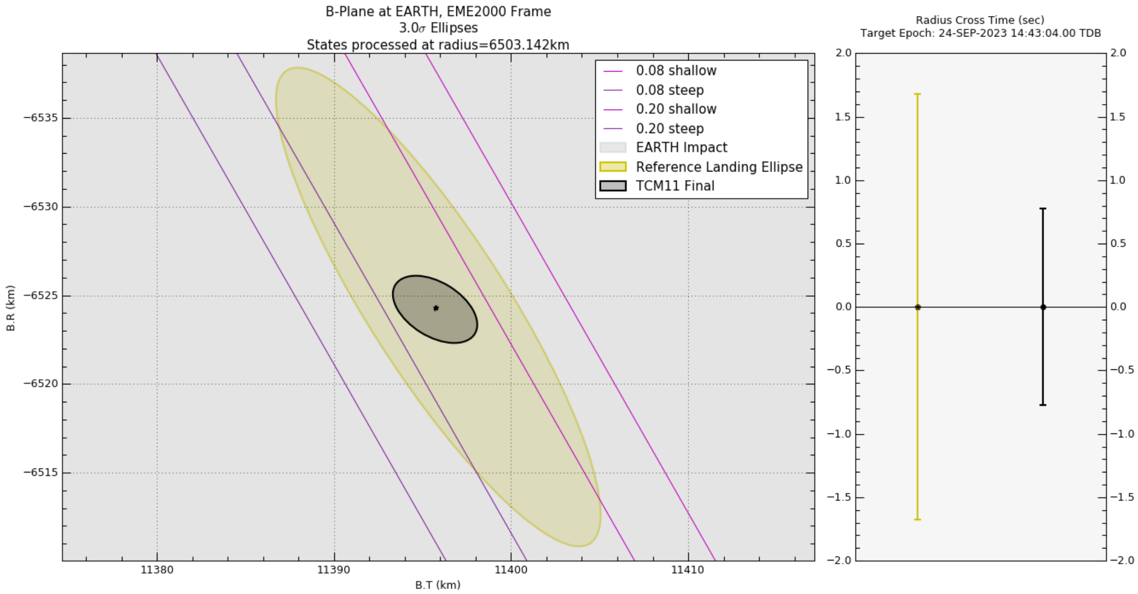

Figure 9: B-Plane plot showing the targeted location of TCM-11 and associated Monte Carlo delivery error ellipse against the mapped reference landing ellipse and $|B|$ contours.

Table 8: TCM-11 Maneuver Parameters and Performance.

TCM-11 Case	Delivery Date	Parameter	Nominal Value	Estimated Value	*A-priori* Sigma	Estimated Sigma	Correction	Correction / *A-priori*
Prelim Design	28-Aug-2023	ΔV, cm/s	23.902	-	-	-	-	-
		RA, deg	211.562	-	-	-	-	-
		Dec, deg	-34.224	-	-	-	-	-
Final Design	08-Sep-2023	ΔV, cm/s	24.000	-	-	-	-	-
		RA, deg	210.902	-	-	-	-	-
		Dec, deg	-34.494	-	-	-	-	-
Initial Reconstruct	11-Sep-2023	ΔV, cm/s	24.000	24.020	0.039	0.030	0.020	0.506
		RA, deg	210.901	211.050	0.135	0.053	0.149	1.102
		Dec, deg	-34.494	-34.615	0.111	0.014	-0.121	-1.082
Final Reconstruct	15-Sep-2023	ΔV, cm/s	24.000	24.039	0.039	0.020	0.033	0.837
		RA, deg	210.901	210.986	0.135	0.084	0.084	0.623
		Dec, deg	-34.494	-34.656	0.111	0.040	-0.161	-1.453

reconstruction no additional new information was available for this design. The initial reconstruct of TCM-11 (Table 8) did show a slight overburn, resulting in a slightly more steep entry trajectory though still well within expected errors. The TCM-12 ΔV to correct for this error was found to be 2.37 mm/s. While still a small correction, the TCM-12 ΔV magnitude was above the 1.5 mm/s criterion, and provided an early indication that TCM-12 would not be waived off. The location of the preliminary TCM-12 trajectory design and the design without a TCM-12 on the B-Plane are provided in Figure 10 in cyan and blue, respectively.

After the preliminary design was delivered to the EDL team on September 11 (E-13 days), it was noted that the nominal solution was predicted to land about 1 km southwest of the center of the target on the ground at UTTR. Upon review, it was found that all the TCM-11 designs also exhibited this behavior though the 1-km shift was not as significant compared to the size of the projected delivery error ellipse at the time. The targeting bias was now more significant with the execution error of TCM-11 realized. In an effort to mitigate the increasingly significant bias, the team began implementing a target shift in order to remove this bias. After a few iterations with the EDL team, a new target set was found that closely centered the target on the ground at UTTR, which is summarized in Table 9. For each day between the TCM-12 preliminary and final designs, the team generated maneuver solutions to both targets to trend the designs, which are summarized in Table 10. By the time of the final design, the project concluded to accept the new target to attempt to remove any inherent bias in the trajectory and so the final design of TCM-12 was targeted only to the new set. This final design showed a ΔV of just over 3 mm/sec and was well within the capability of the LTR thruster suite, and thus was recommended for execution. The B-Plane showing the TCM-12 final design plus associated delivery errors, along with the no burn equivalent are shown in Figure 10 in green and red, respectively. The magnitude of the target shift can be seen as the difference between the centers of the blue (old) and red (new) ellipses in this plot.

Table 9: TCM-12 Target Shift.

Target	γ (deg)	R_{mag} (km)	ϕ (deg)	λ (deg)
Original	-8.2000	6503.142	37.328	-122.812
New	-8.1975	6503.142	37.333	-112.801

TCM-12 executed at the planned time on September 17 (E-7 days). The first reconstruction was available the next day (E-6 days) which showed a slight underburn but overall very good performance for such a small maneuver. The initial reconstruction values are included in the first row of Table 11 and show corrections well below 0.5σ of the *a-priori* maneuver errors, though notably very little information on the ΔV direction was available at that time. Successful execution of this maneuver allowed the team to confidently cancel the contingency TCM-13 opportunity. The team generated daily solutions to trend the predicted location on the B-Plane, which are all shown in Figure 11. The final reconstruction of TCM-12 from the day of SRC Release is provided in Table 11. The final burn performed within 1σ of the predicted errors, though the uncertainty in right ascension did not decrease much despite additional tracking data and several Delta-Differenced One-Way Range (DDOR) measurements throughout the week. A history of the entry conditions for the SRC throughout the entire time period from TCM-11 execution until the full Reconstruction is contained in Table 12.

Starting with the E-5 days solution until E-1 day, the predicted entry location remained relatively

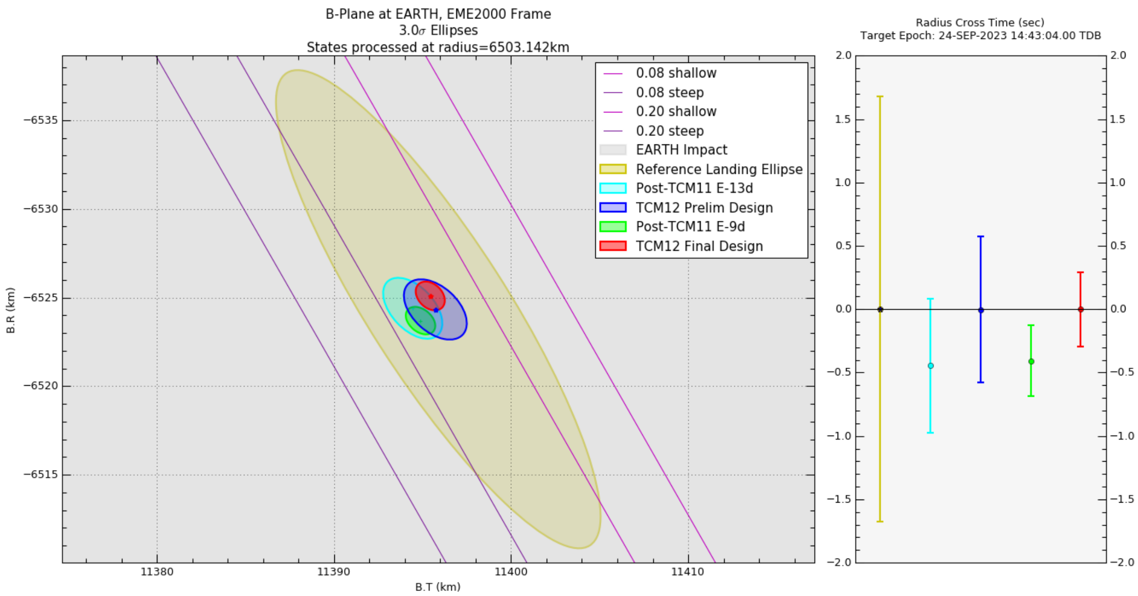

Figure 10: B-Plane plot showing the targeted location of the TCM-12 with burn and no burn trajectories, and associated Monte Carlo delivery error ellipse against the mapped reference landing ellipse and $|B|$ contours.

Table 10: TCM-12 Maneuver Designs.

Design Date	Entry Target	ΔV mm/s	RA deg	Dec deg
11-Sep-2023 (Prelim)	Original	2.380	116.593	12.671
12-Sep-2023	Original	1.787	123.867	48.206
	New	2.755	130.787	77.058
13-Sep-2023	Original	2.299	113.559	34.482
	New	2.962	112.421	63.548
14-Sep-2023	Original	2.263	113.804	41.226
	New	3.056	112.827	68.223
15-Sep-2023 (Final)	New	3.093	111.978	72.288

stable. With no future maneuver planned, a majority of the remaining predicted error was due to uncertainties in the SRC Release ΔV. On E-2 days, the project performed its final conjunction avoidance screening and waived off any potential CAMs, thus TCM-12 was the final maneuver performed for Entry Targeting.

Beginning with the shift to the SRC Release attitude at E-31 hours, outgassing was observed which began to adjust the solution. This is most notable in the sudden change in ellipse center and size beginning at E-7 hr in Figure 11. More details on the outgassing that was observed, and how the reconstruction was performed can be found in Leonard, et al.[7]

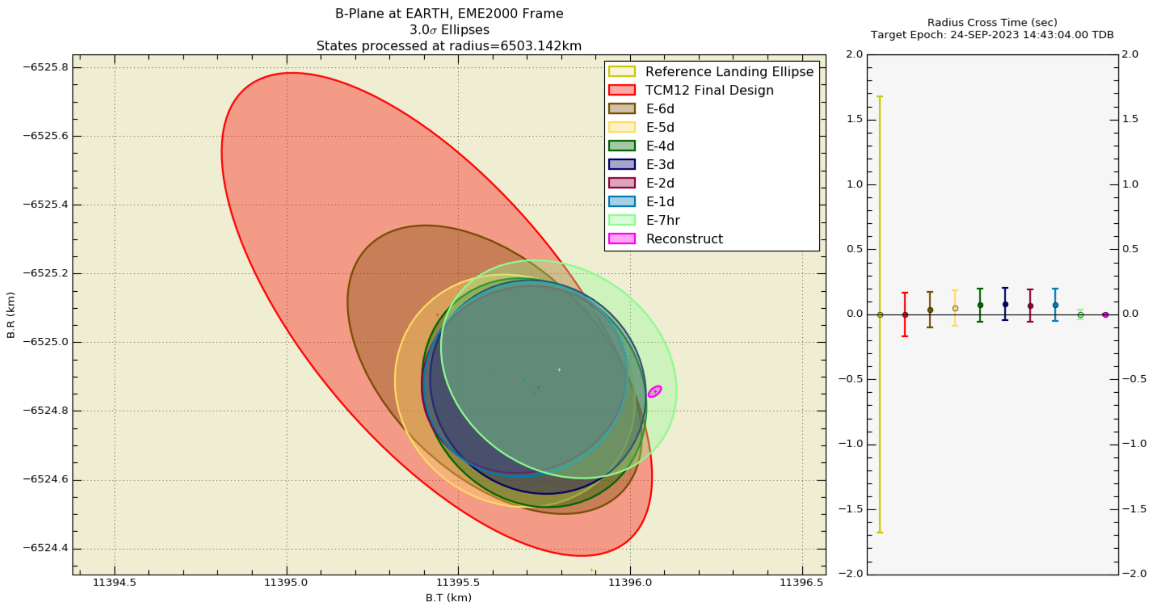

Figure 11: B-Plane plot showing the daily trajectory solutions following TCM-12 until SRC Release with the post-release reconstruct.

Table 11: TCM-12 Maneuver Performance.

TCM-12 Case	Delivery Date	Parameter	Nominal Value	Estimated Value	*A-priori* Sigma	Estimated Sigma	Correction	Correction / *A-priori*
Initial Reconstruct	18-Sep-2023	ΔV, mm/s	3.093	3.008	0.105	0.038	-0.038	-0.359
		RA, deg	111.978	111.491	1.820	1.691	-0.487	-0.268
		Dec, deg	72.288	72.284	0.554	0.553	-0.003	-0.006
Final Reconstruct	24-Sep-2023	ΔV, mm/s	3.093	3.033	0.105	0.032	-0.060	-0.571
		RA, deg	111.978	110.406	1.820	1.432	-1.572	-0.8639
		Dec, deg	72.288	72.185	0.554	0.531	-0.102	-0.185

The final maneuver performed for the primary OSIRIS-REx mission was the Earth Divert. The design of the Divert was delivered along with the TCM-10 final design in July 2023 to provide sufficient time for integration and testing as part of the complex SRC Release sequence. With all activities occurring on schedule as planned, and the Earth flyby delivery error being largely driven by execution error of the Divert burn, little changed in the analysis and predicted trajectory between the time of the final design and execution of the maneuver, which occurred 20 minutes after SRC

Table 12: Atmospheric entry states and uncertainties for each daily solution.

Solution Date	γ_{J2000} (deg) Mean	σ	ϕ_{ECEF} (deg) Mean	σ	λ_{ECEF} (deg) Mean	σ	$V_{mag_{ECEF}}$ (km/s) Mean	σ	χ_{J2000} (deg) Mean	σ
E-14	-8.200	1.85E-02	37.328	1.05E-02	237.188	3.25E-02	12.361	2.68E-05	66.374	1.98E-02
E-13	-8.234	1.26E-02	37.310	7.57E-03	237.130	2.21E-02	12.361	1.89E-05	66.342	1.36E-02
E-12	-8.224	1.01E-02	37.313	5.17E-03	237.148	1.81E-02	12.361	1.76E-05	66.352	1.07E-02
E-11	-8.235	8.41E-03	37.307	4.41E-03	237.128	1.51E-02	12.361	1.49E-05	66.340	8.93E-03
E-10	-8.234	7.38E-03	37.307	4.20E-03	237.130	1.30E-02	12.361	1.19E-05	66.341	7.89E-03
E-9	-8.233	6.75E-03	37.308	4.03E-03	237.133	1.18E-02	12.361	1.01E-05	66.343	7.25E-03
E-8	-8.231	3.57E-03	37.308	2.03E-03	237.136	6.33E-03	12.361	7.39E-06	66.344	3.79E-03
E-7*	-8.197	4.00E-03	37.333	2.36E-03	237.192	7.03E-03	12.361	7.64E-06	66.381	4.26E-03
E-6	-8.195	3.26E-03	37.333	1.94E-03	237.196	5.65E-03	12.361	5.93E-06	66.383	3.48E-03
E-5	-8.195	3.28E-03	37.333	2.05E-03	237.197	5.60E-03	12.361	5.47E-06	66.384	3.53E-03
E-4	-8.193	3.04E-03	37.334	1.92E-03	237.200	5.18E-03	12.361	5.34E-06	66.386	3.27E-03
E-3	-8.193	2.97E-03	37.335	1.86E-03	237.200	5.06E-03	12.361	5.12E-06	66.386	3.19E-03
E-2	-8.194	2.96E-03	37.334	1.85E-03	237.199	5.04E-03	12.361	5.01E-06	66.385	3.18E-03
E-1	-8.194	2.97E-03	37.334	1.86E-03	237.199	5.04E-03	12.361	4.88E-06	66.386	3.18E-03
E-7 hrs	-8.191	7.60E-04	37.335	6.88E-04	237.203	1.52E-03	12.359	6.76E-05	66.388	9.10E-04
Reconstruct	-8.184	9.38E-05	37.339	6.27E-05	237.216	1.88E-04	12.361	5.69E-06	66.396	1.13E-04

* Values are pre-TCM12 execution

Release. The Divert burn executed as planned, with a summary of the burn's performance contained in Table 13, and the reconstructed B-Plane solution against the Monte Carlo analysis shown in Figure 12. The Divert maneuver performed extremely well, and successfully placed the spacecraft on the planned trajectory to begin the OSIRIS-APEX extended mission.

Table 13: Earth Divert Maneuver Performance.

Divert Case	Delivery Date	Parameter	Nominal Value	Estimated Value	*A-priori* Sigma	Estimated Sigma	Correction	Correction / *A-priori*
Reconstruction	20-Oct-2023	ΔV, m/s	65.528	65.487	0.437	6.93E-03	-0.041	-0.094
		RA, deg	56.439	56.377	0.457	1.07E-04	-0.062	-0.136
		Dec, deg	41.700	41.707	0.305	6.56E-05	0.007	0.021

CONCLUSIONS

This paper described the OSIRIS-REx Earth Return and Entry trajectory design, analysis, and execution that led to the successful asteroid Bennu sample return. The trajectory design placed emphasis on spacecraft safety and minimizing risk by guaranteeing the spacecraft trajectory remained away from a possible Earth impact until 14 days prior to entry. The ΔV cost of the return trajectory was minimized by designing specific flybys in the Earth flyby walkdown strategy, which led to a nearly ballistic trajectory design that performed over 99.5% of the total ΔV cost with the initial execution of the asteroid departure maneuver. Detailed modeling of the spacecraft attitude and sample return capsule release in the trajectory designs provided a reliable prediction for the over 2-year return cruise that held close to the as-flown trajectory. Analysis performed by the team heavily leveraged the years of previous flight experience with the spacecraft, but also utilized ample conservatism against uncertain conditions to reliably validate that the design would meet mission requirements and lead to a successful landing. The final maneuvering sequence executed as planned and well within what was analyzed, leading to the cancellation of any contingency maneuvers, and

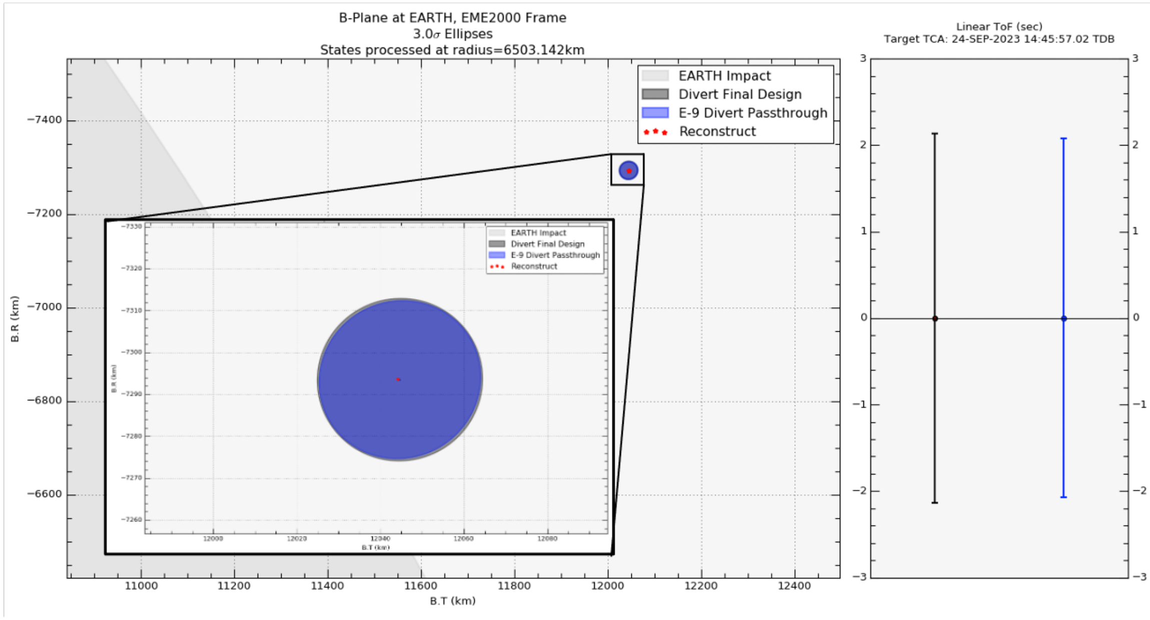

Figure 12: Earth Divert B-Plane showing the as-flown reconstructed trajectory against the 3-sigma expected delivery errors.

ultimately safely landed the sample on the ground in Utah while also placing the spacecraft bus precisely on the trajectory necessary to continue onwards towards Apophis for the OSIRIS-APEX extended mission.

ACKNOWLEDGMENTS

The authors acknowledge members of the OSIRIS-REx team who have contributed to the accomplishments described in this paper: Jason Leonard and other members of the KinetX Orbit Determination team, and the Lockheed Martin flight operations team.

This material is based upon work supported by NASA under Contracts NNM10AA11C and NNG13FC02C. OSIRIS-REx is the third mission in NASA's New Frontiers Program. Dante Lauretta of the University of Arizona, Tucson, is the mission's Principal Investigator, and the University of Arizona also leads the Science Team and the science observation planning and data processing. Lockheed Martin Space Systems in Denver built the spacecraft and is providing flight operations. Goddard Space Flight Center and KinetX Aerospace are responsible for navigating the OSIRIS-REx spacecraft. Contract NNM10AA11C is issued through the New Frontiers Program.

REFERENCES

[1] D. Lauretta, H. Enos, A. Polit, H. Roper, and C. Wolner, "OSIRIS-REx at Bennu: Overcoming challenges to collect a sample of the early Solar System," *Sample Return Missions*, 2021, pp. 163–194.

[2] D. R. Wibben, A. Levine, S. Rieger, J. M. Leonard, C. Adam, L. McCarthy, E. Sahr, D. Nelson, P. G. Antreasian, M. C. Moreau, *et al.*, "OSIRIS-REx post-TAG observation trajectory design and navigation performance," *44th Annual AAS Guidance, Navigation and Control (GN&C) Conference*, No. AAS 22-184, 2022.

[3] D. N. DellaGiustina, M. C. Nolan, A. T. Polit, M. C. Moreau, D. R. Golish, A. A. Simon, C. D. Adam, P. G. Antreasian, R.-L. Ballouz, O. S. Barnouin, *et al.*, "OSIRIS-APEX: An OSIRIS-REx Extended Mission to Asteroid Apophis," *The Planetary Science Journal*, Vol. 4, No. 10, 2023, p. 198.

[4] M. Johnson, E. Queen, A. Williams, S. Dutta, S. Francis, and A. Martinez, "Entry, Descent, and Landing Analysis for the OSIRIS-REx Sample Return Capsule," *46th Rocky Mountain AAS GN&C Conference*, No. AAS 24-188, 2024.

[5] K. M. Getzandanner, P. G. Antreasian, M. A. Shoemaker, J. M. Leonard, D. R. Wibben, K. E. Williams, *et al.*, "OSIRIS-REX Earth Return & Entry: Navigation Operations & Lessons-Learned," *46th Rocky Mountain AAS GN&C Conference*, No. AAS 24-151, 2024.

[6] S. A. Sandford, E. B. Bierhaus, P. Antreasian, J. Leonard, C. K. Materese, C. W. May, J. T. Songer, J. P. Dworkin, D. S. Lauretta, B. Rizk, *et al.*, "Outgassing from the OSIRIS-REx sample return capsule: characterization and mitigation," *Acta Astronautica*, Vol. 166, 2020, pp. 391–399.

[7] J. M. Leonard, M. Q. Myers, B. Page, K. Pipich, C. J. VeNard, P. G. Antreasian, A. Liounis, and K. M. Getzandanner, "OSIRIS-REx Earth Return Orbit Determination Analysis and Performance," *46th Rocky Mountain AAS GN&C Conference*, No. AAS 24-057, 2024.

[8] J. Geeraert, J. Leonard, P. Kenneally, P. Antreasian, , M. Moreau, and D. Lauretta, "OSIRIS-REx Navigation Small Force Models," *Proceedings of the 2019 AAS/AIAA Astrodynamics Specialist Conference*, No. AAS 19-717, American Astronautical Society, 2019, AAS 19-717.

[9] D. Farnocchia, S. Eggl, P. W. Chodas, J. D. Giorgini, and S. R. Chesley, "Planetary encounter analysis on the B-plane: a comprehensive formulation," *Celestial Mechanics and Dynamical Astronomy*, Vol. 131, 2019, pp. 1–16.

[10] G. Kruizinga, J. Seubert, M. Jesick, M. Wong, J. Kangas, E. Gustafson, T. Martin-Mur, T. McElrath, S. E. McCandless, N. Mottinger, *et al.*, "Mars 2020 Navigation Performance," *2021 AAS/AIAA Astrodynamics Specialist Conference*, No. AAS 21-505, August 2021.

[11] G. L. Kruizinga, E. D. Gustafson, P. F. Thompson, D. C. Jefferson, T. J. Martin-Mur, N. A. Mottinger, F. J. Pelletier, and M. S. Ryne, "Mars Science Laboratory Orbit Determination," *23rd International Symposium on Space Flight Dynamics, Pasadena, CA*, 2012.